Quantum Electronics **31** (1) 72 – 78 (2001)

LASER APPLICATIONS AND OTHER TOPICS IN QUANTUM ELECTRONICS

PACS numbers: 42.79.Dj; 42.79.Gn
DOI: 10.1070/QE2001v031n01ABEH001894

Simple method for optimisation of parameters of a combined diffraction grating at grazing incidence

S V Vasil'ev, V A Sychugov

Abstract. **A method for optimising parameters of combined structures consisting of a dielectric diffraction grating and a metal or a multilayer dielectric mirror is proposed. The method is based on the use of waveguide properties of a combined diffraction grating. Its main advantage is that one can determine the optimum parameters of a combined grating without solving the diffraction problem.**

Keywords: *multilayer waveguides, diffraction grating, diffraction efficiency*

1. Introduction

The development of lasers substantially increased requirements to the optical components of laser devices, in particular, the radiation resistance and the efficiency of diffraction gratings. It becomes difficult or even impossible to use conventional metal gratings in the problems aimed at the development of pulsed narrow-band lasers and lasers with a superhigh radiance.

An important step on the way of improving characteristics of diffraction gratings consisted in the development of combined gratings, which were first proposed in Ref. [1]. A schematic diagram of a combined diffraction grating is presented in Fig. 1. A grating G is formed in a dielectric layer deposited on an intermediate dielectric layer S, which, in turn, lies on a metal or multilayer dielectric mirror M. Such gratings have some properties that are important for practice. In Refs [2, 3], combined diffraction gratings with an ultimately high diffraction efficiency and a high radiation resistance are described, which are intended for pulse compression. Refs [4, 5] are devoted to the study of properties of combined diffraction gratings at grazing incidence. As shown in these papers, that of a combined grating with a metal mirror may be substantially higher than that of a conventional grating with a metal coating, with their absorption levels being comparable.

If the wavelength and the angle of incidence of radiation, the refractive indices of materials, and the grating profile are given, the problem of determining parameters of a grating with the maximum efficiency is reduced to the search for optimum values of the grating depth $h^{(G)}$, the intermediate-layer thickness $h^{(S)}$, and, in the case of a grating with a dielectric mirror, the depth of mirror layers $h^{(M)}$. A rigorous solution of the problem of diffraction by a combined grating requires a considerable bulk of calculations. The time required for calculating diffraction efficiencies of grating with prescribed parameters on a modern personal computer ranges from several seconds to several tens of seconds. Our experience of studying combined gratings showed that the dependence of the diffraction efficiency of a grating of this kind on the layer thickness has a large number of local extrema. Because of these factors, the methods of numerical optimisation of parameters of a combined grating with a large number of layers are extremely inefficient.

In this paper, we propose a method that enables one to determine the optimum parameters of a combined diffraction grating in an analytic form or using a considerably smaller computation time than in the case of direct optimisation. The problem is solved by using an approach based on waveguide properties of a combined grating. The waveguide nature of the interaction of light with a combined grating was demonstrated in Ref. [1], which made it possible to obtain an analytic expression for the efficiency of a metal-dielectric combined grating with a small corrugation depth in the autocollimation configuration. Here, we generalise the waveguide approach to the case of more complex structures and arbitrary angles of incidence.

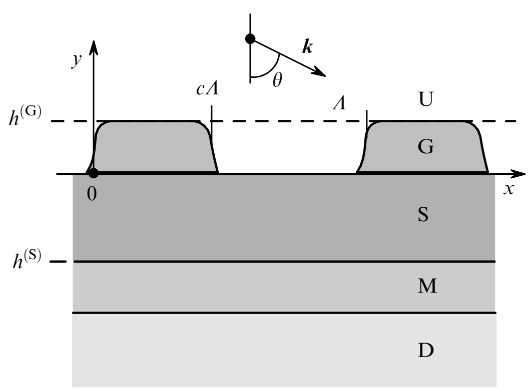

Figure 1. Schematic diagram of a combined grating. (U) upper half-space; (G) diffraction grating layer; (S) matching dielectric layer; (M) metal or dielectric mirror; (D) lower half-space (substrate); ($\boldsymbol{k}$) wave vector of the incident wave; (θ) angle of radiation incidence; (Λ) grating period; (c) grating filling factor.

S V Vasil'ev, V A Sychugov General Physics Institute, Russian Academy of Sciences, ul. Vavilova 38, 117769 Moscow, Russia

Received 21 July 2000
Kvantovaya Elektronika **31** (1) 72 – 78 (2001)
Translated by A Kirkin

2. Interaction of radiation with a combined diffraction grating

In the calculations, we used the so-called modal method of solving the problem of diffraction by a grating. It is described in detail in Ref. [6]. Here, we consider only the basic features of the method, which help us to interpret the results.

Let a plane electromagnetic wave be incident on a grating G from the upper half-space U (Fig. 1). The distribution of the diffraction field should satisfy the Helmholtz equation

$$\left[\frac{\partial^2}{\partial x^2}+\frac{\partial^2}{\partial y^2}+k^2(x,y)\right]F(x,y)=0, \tag{1}$$

the quasi-periodicity condition

$$\exp\left(\mathrm{i}k\Lambda n^{(\mathrm{U})}\sin\theta\right)F(x,y)=F(x+\Lambda,y)\ , \tag{2}$$

and the continuity conditions at the interfaces of spatial regions with different refractive indices. Here, the function $F(x,y)$ coincides with E or H components of the field, depending on the polarisation; $k=2\pi/\lambda$ is the wave number of the incident wave; θ is the angle of incidence of radiation on the grating; and Λ is the grating period.

The solutions of problem (1), (2) in the upper (U) and lower (D) half-spaces are given by the so-called Rayleigh expansions

$$F^{(\mathrm{U})}(x,y)=r^{(\mathrm{i})}\exp\left(\mathrm{i}\alpha_0 x-\mathrm{i}\beta_0^{(\mathrm{U})}y\right)+\sum_{n=-\infty}^{n=+\infty}r_n\exp\left(\mathrm{i}\alpha_n x+\mathrm{i}\beta_n^{(\mathrm{U})}y\right),$$
$$F^{(\mathrm{D})}(x,y)=\sum_{n=-\infty}^{n=+\infty}t_n\exp\left(\mathrm{i}\alpha_n x-\mathrm{i}\beta_n^{(\mathrm{D})}y\right), \tag{3}$$

where $\alpha_n=kn^{(\mathrm{U})}\sin\theta+(2\pi/\Lambda)n$; $\beta_n^{(j)2}=k^2n^{(j)2}-\alpha_n^2$; n is an integer; and $r^{(\mathrm{i})}$ is the amplitude of the incident wave. To the expansion terms with real coefficients, radiative diffraction orders correspond that carry away energy from the grating. The number of such diffraction orders is determined by the ratio of the radiation wavelength to the grating period and, if one considers diffraction into the lower half-space, the refractive index $n^{(\mathrm{D})}$ of the grating substrate.

The solution of problem (1), (2) in the intermediate layer S and layers of the mirror M are also given by the Rayleigh expansions

$$F^{(\mathrm{S,M})}(x,y)=\sum_m\left[a_m^{(\mathrm{S,M})}\exp\left(\mathrm{i}\beta_m^{(\mathrm{S,M})}y\right)+b_m^{(\mathrm{S,M})}\exp\left(-\mathrm{i}\beta_m^{(\mathrm{S,M})}y\right)\right]\exp(\mathrm{i}\alpha_m x). \tag{4}$$

However, in contrast to expansions (3), they contain the terms corresponding to the waves travelling both in the positive and in the negative directions of the y-axis.

If the grooves of the grating have a rectangular profile, one can separate variables in Eq. (1) and obtain the analytic expression

$$F^{(\mathrm{G})}(x,y)=\sum_m\left[a_m^{(\mathrm{G})}\exp(\mathrm{i}\mu_m y)+b_m^{(\mathrm{G})}\exp(-\mathrm{i}\mu_m y)\right]u_m(x) \tag{5}$$

for the field in the grating G. The constants μ_m and the form of the functions $u_m(x)$ in modal expansion (5) can be determined by solving the eigenvalue problem that appears upon integration of Eq. (1) with accounting for the quasi-periodicity condition (2) and continuity conditions for the field and its derivative at the boundary of half-periods (at $x=c\Lambda$, where a constant c is the grating filling factor, see Fig. 1). The coefficients μ_m in (5) and $\beta_n^{(j)}$ in (4) have a similar meaning. The number of real coefficients is limited by the number of radiative diffraction orders, and their value is related to the effective refractive index of the corresponding mode excited by the incident wave in the grating layers G, S, and M.

After obtaining the field expansion in all spatial regions, one uses the continuity conditions at the interfaces of layers of a combined grating and constructs the system of linear equations for the unknown modal amplitudes $a_m^{(j)}$, $b_m^{(j)}$ and the amplitudes of diffraction harmonics r_n, t_n. The solution of this system gives the diffraction efficiency of the grating R_n, T_n in different orders and the phase and intensity of radiation at any point of the space.

3. Interaction of radiation with a multilayer mirror

The interaction of radiation with a multilayer mirror is considerably simpler than the interaction with a diffraction grating, and we consider it in more detail. By using Helmholtz equation (1), we find expressions for the field in all spatial regions:

$$F_{N+1}(x,y)=\left[r\exp(\mathrm{i}\beta_{N+1}y)+r^{(\mathrm{i})}\exp(-\mathrm{i}\beta_{N+1}y)\right]\mathrm{e}(x),$$
$$\vdots$$
$$F_i(x,y)=[a_i\exp(\mathrm{i}\beta_i y)+b_i\exp(-\mathrm{i}\beta_i y)]\mathrm{e}(x), \tag{6}$$
$$\vdots$$
$$F_0(x,y)=t\exp(-\mathrm{i}\beta_0 y)\mathrm{e}(x),$$

where $\mathrm{e}(x)=\exp(\mathrm{i}\alpha x)$; $\alpha=kn_{N+1}\sin\theta$; $\beta_i^2=k^2n_i^2-\alpha^2$; $r^{(\mathrm{i})}$, r and t are the amplitudes of incident, reflected, and transmitted waves, respectively; the subscript '0' specifies the lower half-space, and the subscript '$N+1$' specifies the upper half-space. To find the unknown amplitudes r and t, we use the continuity conditions at the layer boundaries

$$F_i(x,\Sigma_i)=F_{i+1}(x,\Sigma_i),$$
$$\sigma_i F'_{yi}(x,\Sigma_i)=\sigma_{i+1}F'_{yi+1}(x,\Sigma_i), \tag{7}$$

where $\sigma_i=1/\mu_i$ and $\sigma_i=1/\varepsilon_i$ for TE and TH polarisations, respectively; μ_j and ε_j are the magnetic permeability and the permittivity of a medium in the jth spatial region, respectively; and $\Sigma_i=\sum_{j=0}^{j=i}h_j$. Substituting (2) in (3) and making a change of variables, we obtain the system of linear equations

$$
\begin{aligned}
&t=\tilde{a}_1 D_1^- + \tilde{b}_1 D_1^+,\\
&-\xi_0 t=\tilde{a}_1 D_1^- - \tilde{b}_1 D_1^+,\\
&\qquad\vdots\\
&\tilde{a}_i D_i^+ + \tilde{b}_i D_i^- = \tilde{a}_{i+1} D_{i+1}^- + \tilde{b}_{i+1} D_{i+1}^+,\\
&\xi_i(\tilde{a}_i D_i^+ - \tilde{b}_i D_i^-) = \tilde{a}_{i+1} D_{i+1}^- - \tilde{b}_{i+1} D_{i+1}^+,\\
&\qquad\vdots\\
&\tilde{a}_N D_N^+ + \tilde{b}_N D_N^- = \tilde{r} + \tilde{r}^{(\mathrm{i})},\\
&\xi_N(\tilde{a}_N D_N^+ - \tilde{b}_N D_N^-) = \tilde{r} - \tilde{r}^{(\mathrm{i})},
\end{aligned}
\tag{8}
$$

where

$$
\begin{aligned}
&\mathrm{e}_i=\exp(\mathrm{i}\beta_i h_i);\quad \tilde{a}_i=a_i\exp(\mathrm{i}\beta_i\Sigma_{i-1})(\tau_i^+ + \tau_i^-)\tau_i^+;\\
&D_i^\pm=\frac{\tau_i^\pm}{\tau_i^+ + \tau_i^-};\quad \tilde{b}_i=b_i\exp(-\mathrm{i}\beta_i\Sigma_{i-1})(\tau_i^+ + \tau_i^-)\tau_i^-;\\
&\tau_i^\pm=\exp\left(\pm\frac{\mathrm{i}\beta_i h_i}{2}\right);\quad \tilde{r}=r\exp(\mathrm{i}\beta_{N+1}\Sigma_N);\\
&\xi_i=\frac{\sigma_i\beta_i}{\sigma_{i+1}\beta_{i+1}};\quad \tilde{r}^{(\mathrm{i})}=r^{(\mathrm{i})}\exp(-\mathrm{i}\beta_{N+1}\Sigma_N)
\end{aligned}
\tag{9}
$$

and it is assumed that $\Sigma_0=0$. From Eqs (8) follow the recurrent relations that enable one to express all the unknown amplitudes in terms of the incident-wave amplitude:

$$
\begin{aligned}
&\tilde{r}=\frac{\omega_N D_N^+ + D_N^-\chi_N}{\omega_N D_N^+\chi_N + D_N^-}\,\tilde{r}^{(\mathrm{i})},\quad \tilde{b}_{i-1}=\frac{\omega_i D_i^- + D_i^+}{\omega_{i-1}D_{i-1}^+ + D_{i-1}^-}\,\tilde{b}_i,\\
&\tilde{b}_N=\frac{2\,\tilde{r}^{(\mathrm{i})}}{(1+\xi_N)(\omega_N D_N^+\chi_N + D_N^-)},\quad t=\left(\omega_1 D_1^- + D_1^+\right)\tilde{b}_1,
\end{aligned}
\tag{10}
$$

where

$$
\begin{aligned}
&\chi_i=\frac{1-\xi_i}{1+\xi_i};\quad \tilde{a}_i=\omega_i\tilde{b}_i;\quad \omega_1=\mathrm{e}_1\chi_0;\\
&\omega_{i+1}=\mathrm{e}_{i+1}\frac{\omega_i D_i^+ + D_i^-\chi_i}{\omega_i D_i^+\chi_i + D_i^-}.
\end{aligned}
\tag{11}
$$

Thus, the problem is solved. Using expressions (9)–(11), one can find the field amplitude in all spatial regions and, therefore, determine the mirror reflectivity and transmittance R and T.

4. Properties of the simplest combined diffraction grating at grazing incidence

We begin our study of combined diffraction gratings with the case of the simplest structure, which consists only of two layers, namely, a layer in which a grating G with a rectangular profile is formed and a continuos dielectric layer S. Let the refractive indices $n^{(\mathrm{G})}$ and $n^{(\mathrm{S})}$ of the grating and the continuous layer be equal to 1.5 and the refractive indices of the upper and lower half-spaces be equal to unity. The ratio of the radiation wavelength to the grating period is assumed to be 3/2. In this case, the energy is carried away from the grating only in the form of the specularly reflected component and a single diffraction order [the harmonics with numbers 0 and -1 in Rayleigh expansions (3)].

Let us analyse the dependence of the diffraction efficiency of this simplest structure on the parameters $h^{(\mathrm{G})}$ and $h^{(\mathrm{S})}$ for the grating operating at grazing incidence (for the angle of incidence $\theta=89°$). The pattern of the surface levels $R_{-1}(h^{(\mathrm{S})}, h^{(\mathrm{G})})$ is shown in Fig. 2 by gradations of grey. One can see that the dependence has the form of narrow crests, which are periodically positioned on the plane $(h^{(\mathrm{S})}, h^{(\mathrm{G})})$.

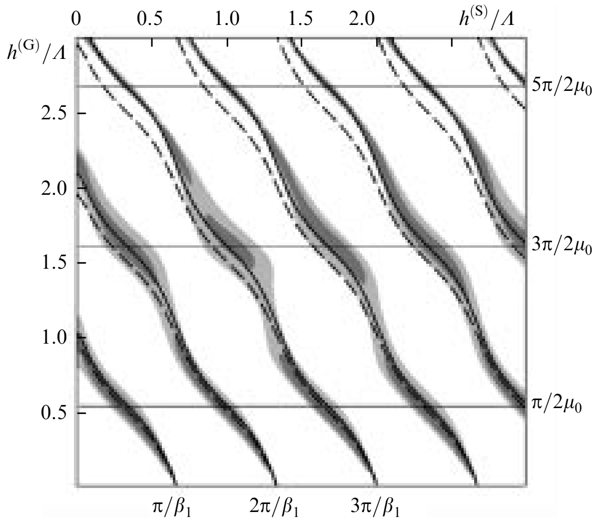

Figure 2. Distribution of levels of diffraction efficiency of a two-layer combined diffraction grating R_{-1} for different values of the grating layer depth $h^{(\mathrm{G})}$ and the dielectric-layer thickness $h^{(\mathrm{S})}$ for grazing incidence of radiation on a grating ($\theta=89°$) (shown by gradations of grey) and the dispersion curves calculated for a two-layer waveguide with $\tilde{n}^{(\mathrm{G})}$ by using Eqn (16) (solid curves) and by the empirical formula (dashed curves).

To analyse the dependence of the diffraction efficiency on the grating depth, we use modal expansion (5). The transverse field distribution in the grating is determined by the factors $\exp(\pm\,\mathrm{i}\mu_m y)$. As noted in Section 3, the set $\{\mu_m\}$ has several (in our case, two) real coefficients μ_0 and μ_{-1}, which may be assigned to the zero and –1st diffraction orders. The field distributions corresponding to these orders are periodic functions of grating depth. Because of this, they should make the dominant contribution to the dependence $R_{-1}(h^{(\mathrm{G})})$. To verify this statement, we introduce the condition

$$
\mu_m h_i^{(\mathrm{G})}=\pi/2+\pi k,\ k=0,1,\ldots,
\tag{12}
$$

which determines the thickness of the quarter-wavelength layer for the mth mode of the grating. The horizontal lines in Fig. 2 are drawn in accordance with condition (12) for the zero grating mode (the coefficient μ_0). One can see that these straight lines pass through the maxima of the dependence $R_{-1}(h^{(\mathrm{S})}, h^{(\mathrm{G})})$. Thus, the form of the dependence $R_{-1}(h^{(\mathrm{G})})$ is determined primarily by the zero grating mode because this mode is most efficiently excited in the case of grazing incidence, whereas condition (12) provides the resonant nature of excitation. Note, however, that other modes of the grating may also have a noticeable effect. For instance, for $h^{(\mathrm{G})}$ at which conditions (12) are fulfilled simultaneously for two modes, the efficiency maxima become sharper (see the upper part of Fig. 2).

Consider now the dependence of the diffraction efficiency on the ratio of the grating depth $h^{(\mathrm{G})}$ to the layer thickness $h^{(\mathrm{S})}$. For this purpose, we replace the grating with a continuous dielectric layer and analyse the interaction of the resulting two-layer mirror $\tilde{\mathrm{G}}\mathrm{S}$ with the incident radiation. Because we have found above that the zero grating mode has the major influence on the diffraction efficiency, we use the coefficient μ_0 for calculating the averaged refractive index $\tilde{n}^{(\mathrm{G})}$ of the layer approximating the grating. For this purpose, we use the relation

$$\mu_0 = k\,\tilde{n}^{(\mathrm{G})}\cos\tilde{\theta} = k\left(\tilde{n}^{(\mathrm{G})2} - \sin^2\theta\right)^{1/2}, \tag{13}$$

where θ is the angle of incidence of radiation on the grating and $\tilde{\theta}$ is the 'angle of refraction' of the incident wave in the approximating layer. The dependence of the refractive index of the approximating layer $\tilde{n}^{(\mathrm{G})}$ on the grating filling factor c, calculated for different angles of incidence, is shown in Fig. 3. The dashed curve presents the dependence obtained by arithmetic averaging $n^{(\mathrm{G})}$ over the grating period: $\tilde{n}^{(\mathrm{G})} = cn^{(\mathrm{G})} + (1-c)$. One can see that the refractive index $\tilde{n}^{(\mathrm{G})}$ at large θ insignificantly differs from the value given by this empirical estimate.

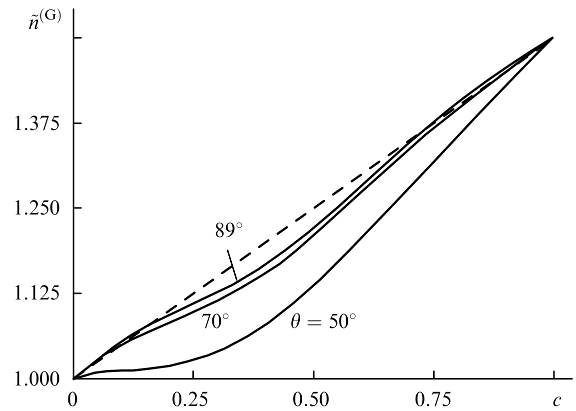

Figure 3. Dependences of the averaged refractive index of the layer approximating a grating $\tilde{n}^{(\mathrm{G})}$ on the grating filling factor c for angles of incidence $\theta = 50°$ (autocollimation regime), 70°, and 89°; the arithmetic averaging of the refractive index over the grating period is shown by the dashed curve.

The condition of grazing incidence allows one to treat the $\tilde{\mathrm{G}}\mathrm{S}$ structure as a two-layer Lummer–Gehrke interferometer or, according to the present-day concepts, as a two-layer dielectric waveguide with weak leakage. It is known that the interaction of radiation with such structures has the resonant nature. The resonance conditions correspond to the maximum of interferometer transmittance or the excitation of a waveguide mode in it. To write the resonance condition in the mathematical form, we use the results obtained in Section 4. Using formulas (9)–(11), we find the relation between the amplitudes of incident and transmitted waves:

$$t = 2r^{(\mathrm{i})}\left\{c_1c_2\left(1+\frac{\beta_0}{\beta_3}\right) - s_1s_2\left(\frac{\beta_1}{\beta_2}+\frac{\beta_0}{\beta_3}\frac{\beta_2}{\beta_1}\right) - \mathrm{i}\left[s_1c_2\left(\frac{\beta_0}{\beta_1}+\frac{\beta_1}{\beta_3}\right)+c_1s_2\left(\frac{\beta_0}{\beta_2}+\frac{\beta_2}{\beta_3}\right)\right]\right\}^{-1}, \tag{14}$$

where

$$c_1 = \cos\left(\beta_1 h^{(\mathrm{S})}\right);\quad s_1 = \sin\left(\beta_1 h^{(\mathrm{S})}\right);$$

$$c_2 = \cos\left(\beta_2 h^{(\mathrm{G})}\right);\quad s_2 = \sin\left(\beta_2 h^{(\mathrm{G})}\right);$$

$$\beta_1 = k\left(n^{(\mathrm{S})2} - \sin^2\theta\right)^{1/2};\quad \beta_0 = k\cos\theta; \tag{15}$$

$$\beta_2 = k\left(\tilde{n}^{(\mathrm{G})2} - \sin^2\theta\right)^{1/2};\quad \beta_3 = k\cos\theta.$$

The phases of the incident and transmitted waves at the maxima of Lummer–Gehrke interferometer transmittance are known to be identical, which means that the imaginary part of the denominator in expression (14) vanishes. Thus, from (14) follows the condition of transverse resonance in the $\tilde{\mathrm{G}}\mathrm{S}$ structure

$$\tan\left(\beta_1 h^{(\mathrm{S})}\right)\left(\frac{\beta_0}{\beta_1}+\frac{\beta_1}{\beta_3}\right) + \tan\left(\beta_2 h^{(\mathrm{G})}\right)\left(\frac{\beta_0}{\beta_2}+\frac{\beta_2}{\beta_3}\right) = 0. \tag{16}$$

Note that expression (16) coincides with the dispersion equation for the dielectric two-layer waveguide with leaky modes, which demonstrates the equivalence of the waveguide approach and the method of description of multilayer structures that was presented in Section 4.

Now we can compare the resonance properties of the combined grating GS and the waveguide $\tilde{\mathrm{G}}\mathrm{S}$. For this purpose, we present in Fig. 2 the dispersion curves corresponding to the solutions of Eqn (16). The solid curves correspond to the dispersion curves of a two-layer waveguide with the refractive index $\tilde{n}^{(\mathrm{G})}$ of the grating layer calculated by relation (13), and the dashed curves are presented for $\tilde{n}^{(\mathrm{G})}$ calculated by the empirical formula. One can see that the dispersion curves almost ideally agree with the crests of the dependence $R_{-1}(h^{(\mathrm{S})}, h^{(\mathrm{G})})$; for gratings of small depth, it suffices to use the empirical estimate of $\tilde{n}^{(\mathrm{G})}$.

Thus, the diffraction efficiency of a two-layer combined grating operating at grazing incidence is high in the case where the condition of double resonance is fulfilled: the condition of excitation of a waveguide mode in the structure approximating the combined grating (16) and the condition of resonance in the diffraction grating layer (12). Note that an increase in the refractive index of the grating material causes an increase in the number of real coefficients in the set $\{\mu_m\}$, i.e., an increase in the number of transverse modes being excited. This adds complexity to the interaction of radiation with a grating and hampers the application of our method.

5. Optimisation of parameters of a combined grating with a metal mirror

Using the results obtained for the simplest model of a combined grating, we can pass to the study of more complex structures that are of greater importance for practice. Actual diffraction gratings are deposited on a substrate. To lower the leakage of radiation from a combined grating to the substrate and, therefore, provide the possibility of resonance interaction of radiation with a grating, one can use a metal or a dielectric mirror (see Fig. 1). Consider a combined grating in which a metal film is used as a metal mirror M. Let the parameters of the problem be as follows: the grating period $\Lambda = 1000$ nm, the radiation wavelength $\lambda = 1500$ nm, the angle of incidence $\theta = 89°$, $n^{(G)} = n^{(S)} = 1.5$ (quartz), $n^{(M)} = 1.4 + i15$ (aluminium), and the grating is assumed to have a rectangular profile with the filling factor $c = 0.5$.

The dependence $R_{-1}(h^{(S)}, h^{(G)})$ for the grating with the aluminium mirror is presented in Fig. 4. The levels of the surface $R_{-1}(h^{(S)}, h^{(G)})$ are shown by gradations of grey, and the regions of high grating absorption are dashed. Let us repeat for this grating the procedure of determining the optimum values of $h^{(G)}$ and $h^{(S)}$, which was described above. The refractive index of the upper layer, which approximates the waveguide grating, will be found from relation (13). Because the refractive index of the substrate underlying the waveguide is complex, one cannot separate out in the explicit form the real and imaginary parts in expression (14). Therefore, the dispersion equation for a two-layer waveguide on a metal substrate takes the form

$$\mathrm{Im}\left\{c_1 c_2\left(1+\frac{\beta_0}{\beta_3}\right) - s_1 s_2\left(\frac{\beta_1}{\beta_2}+\frac{\beta_0}{\beta_3}\frac{\beta_2}{\beta_1}\right) - \mathrm{i}\left[s_1 c_2\left(\frac{\beta_0}{\beta_1}+\frac{\beta_1}{\beta_3}\right) + c_1 s_2\left(\frac{\beta_0}{\beta_2}+\frac{\beta_2}{\beta_3}\right)\right]\right\} = 0. \quad (17)$$

The solutions of this equation, corresponding to the excitation of waveguide modes in the $\tilde{\mathrm{G}}$SM structure, are shown in Fig. 4 by solid curves. The values of grating depth that satisfy conditions (12) are specified by the horizontal straight lines. One can see that the dispersion curves pass through the regions of high diffraction efficiency. Thus, in the case of a metal mirror, the waveguide properties of a combined grating are retained.

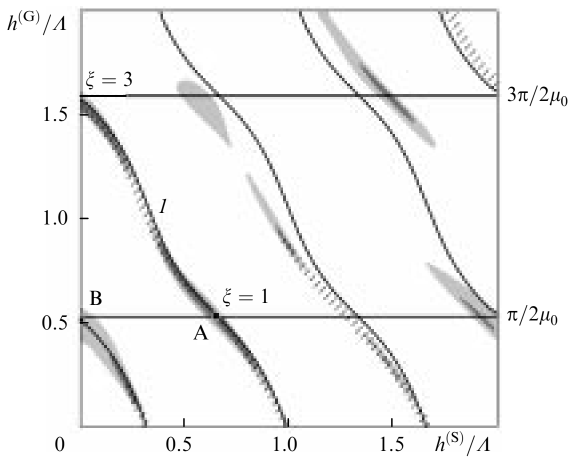

Figure 4. Distribution of levels of diffraction efficiency (shown by gradations of grey) and regions of high light absorption (dashed regions) of a metal-dielectric combined grating for different values of the grating layer depth $h^{(G)}$ and the dielectric-layer thickness $h^{(S)}$ for $\theta = 89°$, $\Lambda = 1000$ nm, $\lambda = 1500$ nm, and $c = 0.5$ and the dispersion curves of a waveguide (solid curves).

In the case where one determines the optimum parameters of a metal-dielectric combined grating, the level of radiation absorption is of no less importance than the diffraction efficiency. One can see from Fig. 4 that the regions of high grating absorption coincide with resonances in the $\tilde{\mathrm{G}}$SM waveguide. Fig. 5 illustrates changes in the diffraction efficiency and the ratio of grating absorption to its efficiency with changing position of the point $(h^{(S)}, h^{(G)})$ on the dispersion curve (curve *1* in Fig. 4). On the abscissa the conventional coordinate ξ is plotted, and the value $\xi = 1$ corresponds to the first resonance in the grating layer, whereas $\xi = 3$ corresponds to the second resonance. One can see from Fig. 5 that the grating efficiency somewhat decreases at the points of double resonance ($\xi = 1$, 3), but the absorption-to-efficiency ratio reaches a minimum at these points. At the points $\xi = 0$ and 2, we have the lowest grating efficiency and resonance absorption.

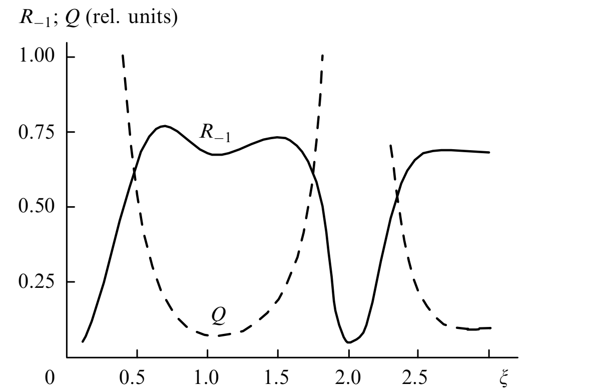

Figure 5. Dependences of the diffraction efficiency R_{-1} and the absorption-to-efficiency ratio of a metal-dielectric combined grating on the position of a point $(h^{(S)}, h^{(G)})$ on the dispersion curve *1* (see Fig. 4).

Thus, the optimisation method proposed here is quite efficient for combined gratings with a metal mirror. Using the condition of double resonance, one can determine parameters of a grating with a high efficiency and the optimum efficiency-to-absorption ratio.

At the end of this section, we consider the effect of geometrical characteristics of a grating on the width of the spectral region where the grating has a high efficiency. Fig. 6

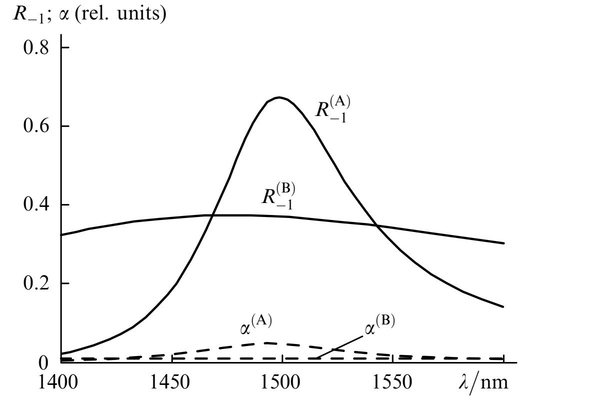

Figure 6. Dependences of the diffraction efficiency R_{-1} and absorptance α of a metal-dielectric grating on the radiation wavelength λ for the grating parameters corresponding to points A and B (Fig. 4).

presents the dependences of the diffraction efficiency of a grating on the radiation wavelength for two lowest resonances (labelled A and B in Fig. 4). One can see that the diffraction efficiency of the grating with the minimum thickness of the intermediate layer (point B) is relatively low, but its spectral range is rather wide. For the grating parameters corresponding to the point A, resonance properties of the grating are pronounced stronger, which leads to an increase in diffraction efficiency and the narrowing of the efficiency peak on the wavelength scale.

6. Combined gratings with a multilayer dielectric grating

The main disadvantages of combined diffraction gratings with a metal mirror are a low radiation resistance and a noticeable absorption level, which are caused by a finite metal conduction. Because of this, of greatest interest for practice are combined gratings with a multilayer dielectric mirror. In the simplest case, one can use a mirror consisting of alternating quarter-wavelength layers with high and low refractive indices. It is known that the thickness h of this mirror is determined from the condition

$$h\left(n^2 - \sin^2\psi\right)^{1/2} = \frac{\lambda}{4}\,, \qquad (18)$$

where λ is the radiation wavelength; n is the refractive index of the layer; and ψ is the angle of incidence on the mirror. Our calculations showed that a concrete value of the angle ψ has no decisive influence on the properties of a combined grating.

Fig. 7 presents the dependences of the maximum diffraction efficiency of a combined grating on the number N of layers for ψ equal to the angle of incidence on the grating $\theta = 89°$ the diffraction angle $\varphi = 30°$, and the average arithmetic of the angle of incidence and the diffraction angle. The maximum of the grating diffraction efficiency was determined by direct numerical optimisation. The grating G and the intermediate layer S had refractive indices of 1.5, the mirror layers had refractive indices of 1.5 and 2.5, and the remaining parameters of the problem were the same as in Section 5. One can see from Fig. 7 that the efficiency of a combined diffraction grating rapidly increases with increasing number of layers N and virtually reaches its maximum value for $N \geqslant 20$. The best characteristics are obtained for the grating with $\psi = (\theta + \varphi)/2$. It is likely that this is caused by the fact that the mirror in this case has the highest reflectivity both for the incident and for the diffracted radiation.

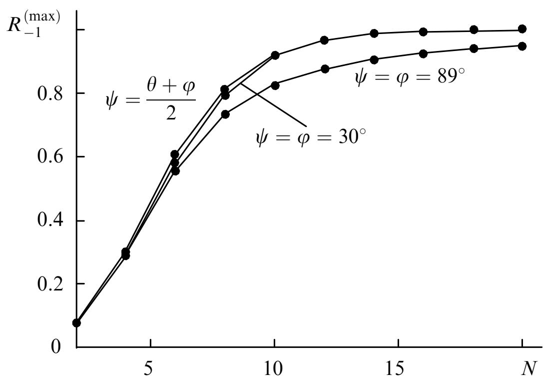

Figure 7. Dependences of the maximum diffraction efficiency $R_{-1}^{\max}$ of a combined grating with a multilayer mirror on the number of mirror layers N for the angles of incidence on the mirror $\psi = \theta = 89°$, $\psi = \varphi = 30°$, and $\psi = (\theta + \varphi)/2$.

Fig. 8 presents the pattern of levels of the surface $R_{-1}(h^{(S)}, h^{(G)})$ for the combined grating with the number of mirror layers $N = 20$ and the angle $\psi = (\theta + \varphi)/2$. The corrugated layer of a combined grating is approximated by a continuous dielectric layer. As the number of layers is increased, it becomes difficult to obtain analytical expressions for radiation transmitted through and reflected from the mirror. Because of this, the mirror parameters were determined numerically, using recurrent relations (10) and (11), which were obtained in Section 4.

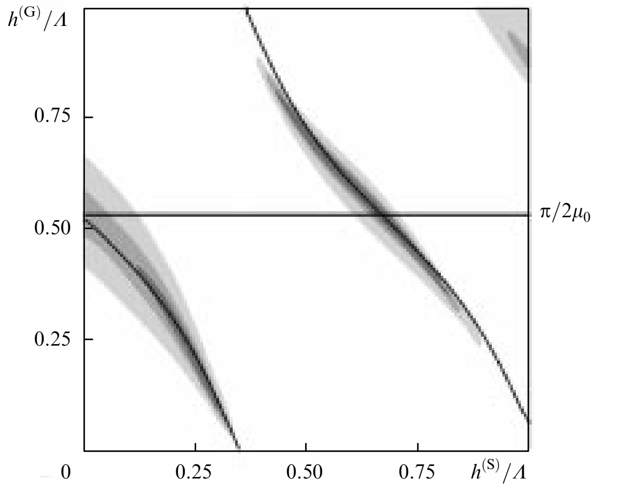

Figure 8. Distribution of levels of diffraction efficiency R_{-1} of a combined grating with a multilayer mirror for different values of parameters $h^{(G)}$ and $h^{(S)}$; the number of mirror layers $N = 20$; and the angle of radiation incidence on the grating $\psi = (\theta + \varphi)/2$.

The solid curves in Fig. 8 show the regions of values of $h^{(G)}$ and $h^{(S)}$ at which the incident wave and the wave transmitted through the mirror have the same phase, i.e., the transverse-resonance condition is fulfilled. One can see that in the case of a large number of dielectric layers the waveguide resonances also coincide with the regions of high diffraction efficiency.

Fig. 9 presents the spectral dependences of the diffraction efficiency of combined gratings with different number of mirror layers N. The angle of radiation incidence on a grating is 89°. In this case, the diffraction efficiency of the combined grating with a multilayer mirror reaches 100%, which is several-fold higher than the efficiency of a conventional grating with a metal coating (shown by the dashed line). The peaks of diffraction efficiency of the dielectric combined grating are narrower than the peaks of the metal-dielectric grating (see Fig. 6). It is likely that one can overcome this disadvantage of a purely dielectric grating by using a complex choice of parameters of a multilayer mirror.

When analysing properties of combined gratings, we restricted our consideration to the case of grazing incidence of radiation. From the viewpoint of the waveguide appro-

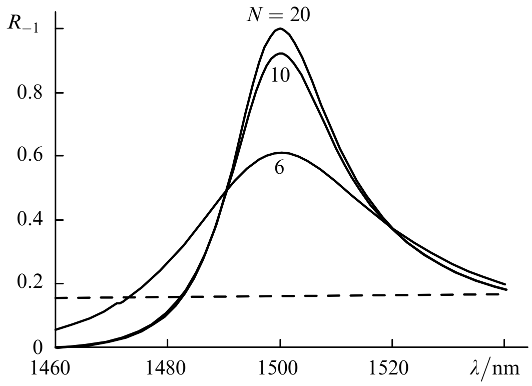

Figure 9. Spectral dependences of the diffraction efficiency R_{-1} of combined gratings with multilayer mirrors having different number of levels N; the dashed line presents the dependence for an aluminium grating with a sine profile.

ach, this illumination scheme provides low leakage in a waveguide and, therefore, the resonance nature of interaction of radiation with a grating and its waveguide properties are best pronounced. However, our approach appears to be quite suitable for the study of combined gratings for different conditions of radiation incidence.

Fig. 10 presents the pattern of levels of the surface $R_{-1}(h^{(S)}, h^{(G)})$ for the dielectric combined grating working in the autocollimation scheme. The results are presented for the number of layers $N = 20$ and $\psi = \theta \approx 49°$; the remaining parameters are the same as in Fig. 8. The solid curves show the regions of excitation of waveguide modes of a multilayer waveguide, with the refractive index of the approximating layer $\tilde{n}^{(G)}$ corresponding to the coefficient μ_0 in expansion (5), and the dashed curves correspond to the coefficient μ_{-1}. It follows from Fig. 10 that the waveguide nature of interaction of radiation with the grating is retained even for a noticeable deviation from grazing incidence. However, in this case, different modes excited in the grating layer manifest their effect in the same extent.

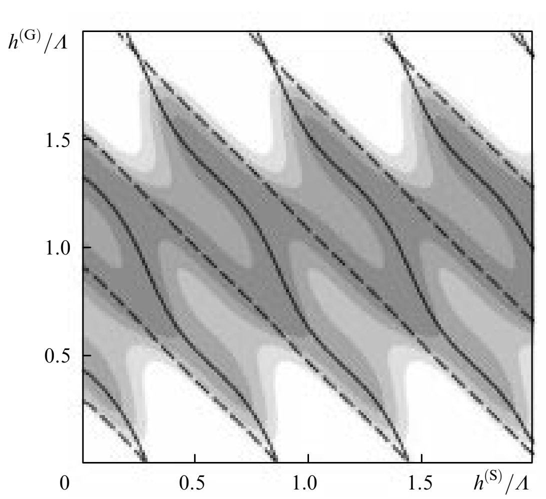

Figure 10. Distribution of levels of diffraction efficiency R_{-1} of a combined grating with a multilayer mirror working in the autocollimation scheme ($\psi = \theta = 49°$) for different values of parameters $h^{(G)}$ and $h^{(S)}$.

7. Conclusions

Our study of the properties of combined diffraction grating, which was made on the basis of the modal approach to the solution of the diffraction problem, showed that the highest diffraction efficiency of a grating operating at grazing incidence is caused by the formation of transverse resonances in a combined structure. The resonance properties of a combined grating were found to be equivalent to the properties of a dielectric waveguide. Using the coincidence of resonance properties of a grating and the waveguide approximating it, one can determine the optimum parameters of a combined grating by solving the dispersion equations for layered structures rather than the diffraction problem, which qualitatively simplifies the optimisation procedure.

It is shown that the waveguide nature of interaction of a radiation with a combined grating manifests itself not only at grazing incidence, but also in other configurations, for instance, in the autocollimation scheme.

The use of an analogy between the properties of a grating and a waveguide seems to offer the greatest promise for the study and optimisation of gratings combined with a multilayer dielectric mirror because the direct numerical optimisation of such structures is a complicated problem.

Acknowledgements. We are grateful to B A Usievich and S K Borisov for useful discussions. This work was supported by the Russian Foundation for Basic Research, Grant No. 00-02-17442.

References

1. Svakhin A S, Sychugov V A, Tikhomirov A E *Zh. Tekh. Fiz.* **61** (9) 124 (1991)
2. Perry M D, Boud R D, Britten J A, Decker D, Shore B W, Shannon C, Sults E *Opt. Lett.* **20** 940 (1995)
3. Shore B W, Perry M D, Britten J A, Boud R D, Feit M D, Nguyen H T, Chow R, Loomis G E, Lifeng Li J. *Opt. Soc. Am. A* **14** 1124 (1997)
4. Salakhutdinov I F, Sychugov V A, Par'e O *Kvantovaya Elektron.* **25** 1009 (1998) [*Quantum Electron.* **28** 983 (1998)]
5. Vasil'ev S V *Kvantovaya Elektron.* **25** 429 (1998) [*Quantum Electron.* **28** 416 (1998)]
6. Botten I C, Craig M S, McPhedran R C, Adams J L, Andrewartha J R *Opt. Acta* **28** 413 (1981)